Numerical and Experimental Study of a Surging Point Absorber Wave Energy Converter

M.A. Bhinder[1], C.G. Mingham[1], D.M.Causon[1], M.T. Rahmati[2], G.A. Aggidis[2] and R.V.Chaplin[2]

[1] Department of Computing and Mathematics,
Manchester Metropolitan University,
Chester Street, M1 5GD Manchester, UK
E-mail: m.bhinder@mmu.ac.uk

[2] Renewable Energy Group,
Faculty of Science and Technology,
Lancaster University, LA1 4YR Lancaster, UK
E-mail: m.rahmati@lancaster.ac.uk

Abstract

Numerical modeling of a WEC is presented in this paper along with some details of the experimental setup. Issues related to the numerical modeling of the single DOF (degree-of-freedom) motion of a surging point absorber WEC (wave energy converter) are outlined and a comparison with experimental data is presented. A commercial CFD code Flow-3D has been used for the numerical modelling and the ability of the code to simulate free surface linear waves and wave structure interaction is evaluated in this paper.

The work is aimed at simulating a surging wave energy converter to achieve an optimized shape and to predict output power at a higher or full scale. The findings of this study may also serve as a reference point for the use of a commercial code such as Flow-3D for simulating such problems.

Keywords: CFD, Numerical modeling of Wave Energy Converter, Flow-3D, Surging Point absorber.

1 Introduction

As a renewable energy source, wave energy has received considerable interest from the research and industrial sectors over the past three decades. The recent quest to address global warming has fueled research in this important source of renewable energy. As a result, a great many prototypes have been proposed and are being tested both experimentally and numerically.

Research at Lancaster University has been mainly concentrated on the invention and development of novel point absorber WECs at model scale which has led to increased understanding of the theory and systematic design of these devices [1-2]. Point absorbers, which were first investigated by [3-4], appear potentially more economical compared to other wave energy converters. However, a surging point absorber appears to have twice the output power compared to heaving device as described by [4].

WRASPA (Wave-driven, Resonant, Arcuate action, Surging Point-Absorber) is a novel pitching surge WEC which has been developed at Lancaster University and is intended to be deployed at water depths of 20-50 meter. In this device, wave forces act on the face of a collector body carried on an arm that rotates about a fixed horizontal axis below sea level. Accordingly, the body oscillates at about the frequency of the ocean swell generating high power from a small and relatively cheap device. In storms the arm automatically moves to a position that minimises forces and so ensures its survival. The experimental and numerical results show that pitching-surge point-absorber WECs have the potential to generate high power from relatively small devices [5-9]. This paper focuses on the recent results of an experiment and numerical study of WRASPA.

Numerical study of a WEC has a potentially great impact on possible design changes at an early stage in the model design. Several design configurations can be tested numerically at a much lower cost compared to an experimental setup. Major issues, however, related to numerical modeling of such devices include proper handling of the free-surface interface, wave-structure interaction and wave reflection at wall boundaries. A diagram showing the collector body which rotates around a specified pivot is shown in Fig. 1.

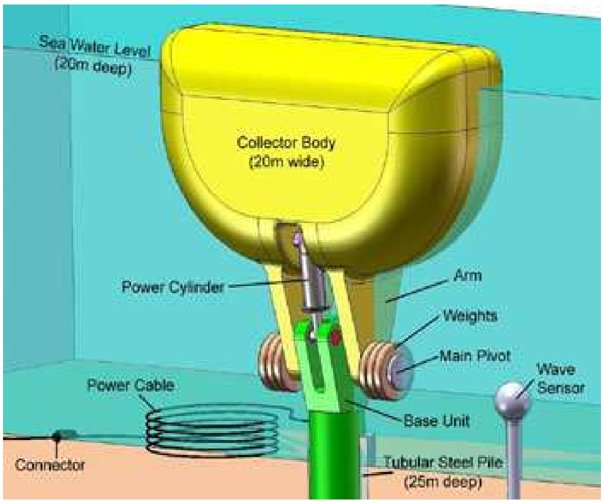

Figure 1: Collector body of WRASPA.

Text within the body of the paper should be in 10 pt Times New Roman, single spaced. Text should be justified. Variations of font (e.g. italics, small portions of sans-serif fonts) may be used for emphasis within the paper but not in underline mode. Please do not use these variations for extended portions of the paper.

On the last page, the authors should try to balance the text between both columns.

2 Wave Tank Experiments

Small scale tank tests of WRASPA have been performed by the experimental project partner Lancaster University UK. The experimental findings of both free and controlled motion of the device, in linear and non-linear waves, has led to an improved understanding of WRASPA's interaction with incoming waves.

A stepwise control system has also been devised for extracting optimum power from irregular waves [10]. Wave gauges have been used to monitor free surface elevation, and the required braking torque, based on automatic switching, has been used to supply the control torque. The power take off system matches the wave forces at various conditions in order to capture maximum power.

It is found that maximum power is obtained when the device is tuned according to the incoming wave swell. At this tuning the natural frequency of the device is adjusted to the incoming wave frequency. Decay tests have been carried out to measure WRASPA's natural frequency. In the decay tests the device is pulled in still water toward maximum displacement and then released while recording the time history of its position.

The experimental study revealed that changing the freeboard or pivot depth controls the natural frequency of the device. Thus, this serves as an easy way of tuning the device according to the desired frequency spectrum [10].

Wave tank tests have been carried out at Lancaster University on a 1/100th scale model of the device to evaluate its performance. The model and apparatus used are shown in (Fig. 2). The collector body has a streamlined shape to permit large amplitude motion to extract energy from the waves [6-7]. The wave force vector on the collector and the pitch of the device were measured for various body immersions and pivot depths.

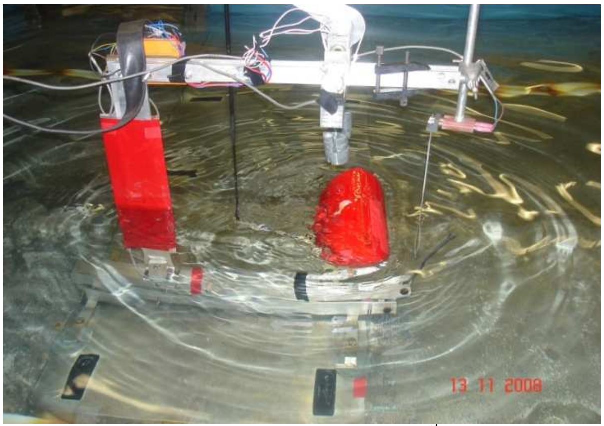

Figure 2: Experimental apparatus of 1/100th scale model of WRASPA

3 Numerical Modelling

Numerical modeling of such devices not only ensures that the current experimental results are validated but also provides an in-depth view of the underlying complex phenomenon of wave structure interaction. It also helps in predicting projected yields from a higher scale model that clearly offers huge advantages for experimental and development teams. Using numerical tools the design of a wave energy converter can be optimized to a higher standard providing improved maximum output power at a relatively lower cost.

Mathematically, the Navier-Stokes equations are used to describe the fluid flow and rigid body motion. This system of partial differential equations can be solved analytically only for simple flow problems. However, for complex problems, algebraic approximations are needed to solve the equations numerically.

In this paper, the presented numerical results are based on the use of a commercial CFD (computational fluid dynamics) package Flow-3D, a product of Flow Science Inc. In a preliminary analysis a number of commercial codes were considered for the purpose of modeling WRASPA but Flow-3D was found to be a good choice for this particular problem, as discussed in [11]. Flow-3D is based on the Reynolds Averaged Navier Stokes (RANS) Equations. To capture the free-surface interface a technique named TruVOF is implemented within Flow-3D. This technique does not need extra cells at the free surface and hence reduces the computation time significantly.

Flow-3D uses a unique technique named FAVOR™ to describe geometric objects in a computational domain which is based on the concept of area fraction (AF) and volume fraction (VF) on a rectangular structured mesh [12]. The FAVOR[TM] technique works well with complex geometries by introducing the effects of AF and VF into the conservation equations of fluid flow. This technique has led to the successful development of a general moving object (GMO) capability which in principle permits the modeling of any type of rigid body motion (six degree of freedom, fixed axis and fixed point) on a fixed-mesh.

A fixed axis dynamically coupled motion of WRASPA has been modeled by implementing this GMO capability of Flow-3D. The flow solver calculates the AF and VF at each time step to describe accurately the object's position on a fixed-rectangular mesh. Hydraulic, gravitational, and control forces and torques are calculated and the equations of motion for the rigid body are solved explicitly for the translational and rotational velocities of moving objects under coupled motion. Further details of the mathematical model used within Flow-3D are given in the next sub-section.

Equations of Motion for Moving Rigid Body in Flow-3d

For 6-DOF motion, the GMO model considers a moving body's centre of mass G as the base point. The equations of motion governing the two separate motions, namely translational and rotational, are [13]

$$\vec{F} = m\frac{d\vec{V_G}}{dt} \qquad (1)$$

$$\vec{T_G} = [J].\frac{d\vec{\omega}}{dt} + \vec{\omega}\times\left([J].\vec{\omega}\right) \qquad (2)$$

where F is the total force, m is rigid body's mass, V_G is mass centre velocity, T_G is the total torque about G and $[J]$ is moment of inertia tensor about G in a body fitted reference system. The total force and total torque are calculated as the sum of several components as

$$\vec{F} = \vec{F_g} + \vec{F_h} + \vec{F_c} \qquad (3)$$

$$\vec{T_G} = \vec{T_g} + \vec{T_h} + \vec{T_c} \qquad (4)$$

where $\vec{F_g}$ is the gravitational force, $\vec{F_h}$ is the hydraulic force due to the pressure field and wall shear forces on the moving object, $\vec{F_c}$ is the net control force prescribed to control or restrict the rigid body's motion. Similarly, $\vec{T_G}, \vec{T_g}, \vec{T_h}$ and $\vec{T_c}$ are the total torque, gravitational torque, hydraulic torque and control torque about the mass centre respectively.

Full details of the underlying conservation equations and mathematical model used for GMO are given in [14].

Simulation Setup in Flow-3d

The geometry file of the device was imported in STL format into the computational domain. It was observed that the geometry file and mesh structure can be modified independently reducing the problem setup time significantly. Three different mesh configurations were tested for mesh-independence and an optimum mesh was selected.

To add extra cells in a region of critical flow behaviour, the option exists to use a nested mesh block. The mesh structure together with the boundary conditions used is shown in Fig. 3.

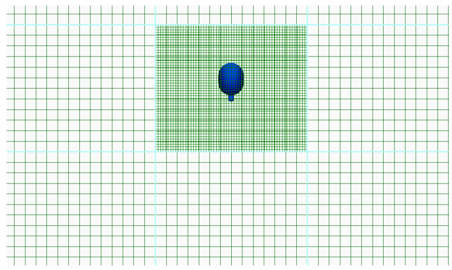

Figure 3: Side view of the computational domain showing mesh and boundary conditions.

The side wall boundaries in Fig. 3 were chosen to be symmetry boundaries. A linear wave boundary condition is set by prescribing velocity components using linear wave theory. The turbulence model used for the final simulations was the RNG (Renormalization group) model preferred by [14].

An implicit GMO model was used for all simulations. It was observed that the implicit method displayed high stability and good efficiency compared to the explicit model.

4 Results

A linear wave was modeled in the NWT (numerical wave tank) as part of a preliminary analysis and the resulting wave propagation was studied. It is observed that Flow-3D's solver is quite robust and efficient while modeling waves. The specification of the simulated wave is given below whereas the surface elevation of this wave at two different locations is presented in Fig. 4.

Wave amplitude = 0.15m, Time period = 4.2s, Water Depth = 1.5m, Tank Dimensions = (35m, 1.5m, 2.5m),

Computational Specifics = Intel(R) Core(TM)2 Duo CPU E6750@2.66GHz , 8GB of RAM.

Total Number of Cells = 793638, Smallest Cell Size = 5.4773E-02

Time taken by solver to compute a 20 seconds case = 2.030E+04(seconds) = 5.63 hr

(a)

(b)

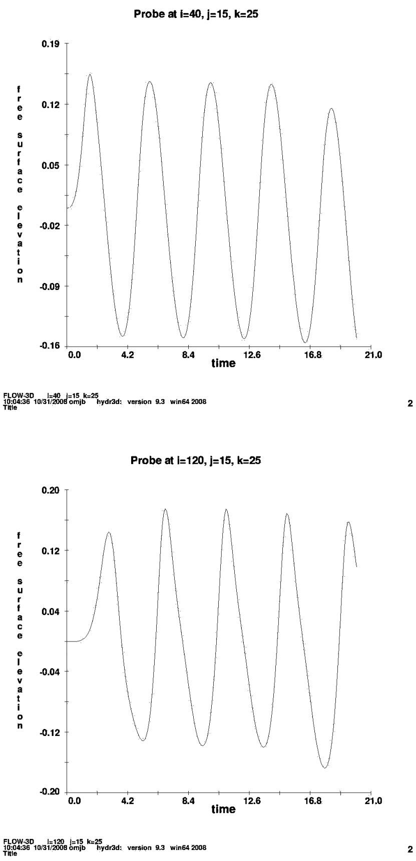

Figure 4: Surface elevation at (a) x=2.1m (b) x=6.5m.

Experimental results of the decay test are validated by comparison with numerical results as plotted in Fig. 5.

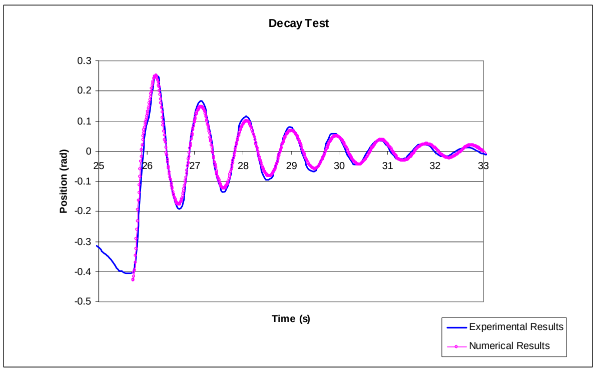

Figure 5: Comparison of experimental and numerical results of decay test.

To model the decay tests, two separate simulations were setup. In the first simulation, the device was pulled towards one end up by 0.4 rad. This was achieved by prescribing a constant velocity. Then in the second simulation the coupled motion of WRASPA was simulated by using the results file of first simulation as initial conditions.

The pitch motion of the device for a range of linear waves was modeled and the results compared with the experimental data (Fig. 6~7).

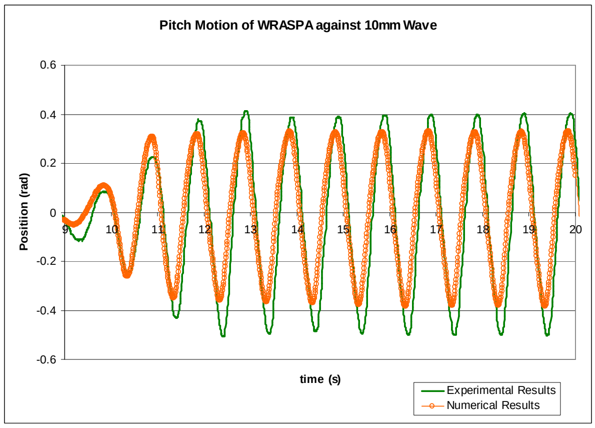

Figure 6: Pitch motion of WRASPA against linear wave of 10 mm Amplitude.

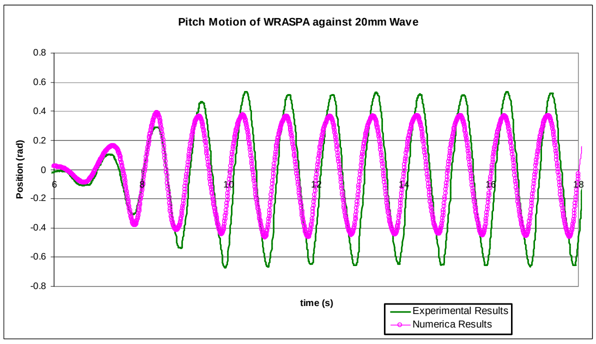

Figure 7: Pitch motion of WRASPA against linear wave of 20 mm Amplitude.

As part of the shape optimization process, two collector shapes were tested numerically as depicted in Fig. 8.

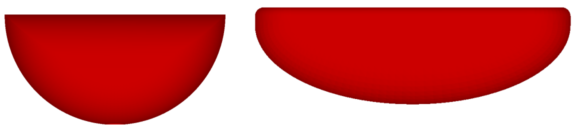

(a) (b)

Figure 8: Front view of two collector shapes (a) RHM1 (b) RHM2.

In the modeling of the decay tests for each shape the natural frequency was tuned according to the incoming wave. The simulated pitch motion of RHM2 is currently being analyzed experimentally.

The torque was measured numerically for both shapes during the characterization tests and compared (Fig. 9) in order to distinguish an optimum shape.

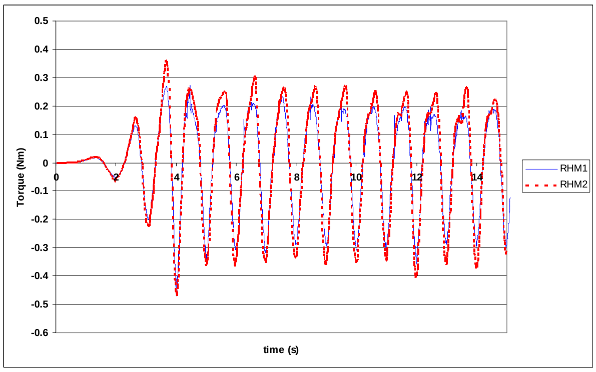

Figure 9: Numerical Results of time history of torque for both shapes monitored in the characterization tests.

Visual comparison of experimental and numerical output is shown in (Fig. 10).

(a)

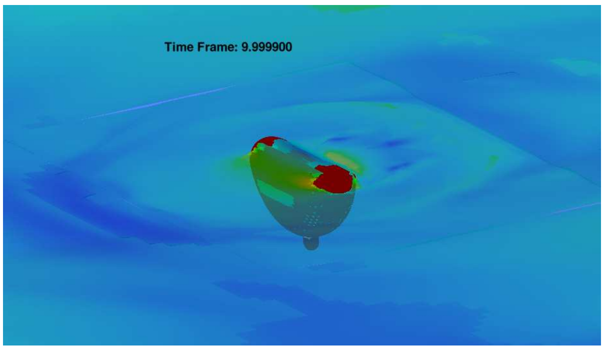

(b)

Figure 10: WRASPA in action (a) Experimental wave tank (b) Numerical wave tank.

Furthermore, the numerical results of the characterization tests are compared to the experimentally measured data (Fig. 11). In these tests the collector body is forced to remain still while waves of varying amplitude are passed over it and the net control torque of the collector monitored.

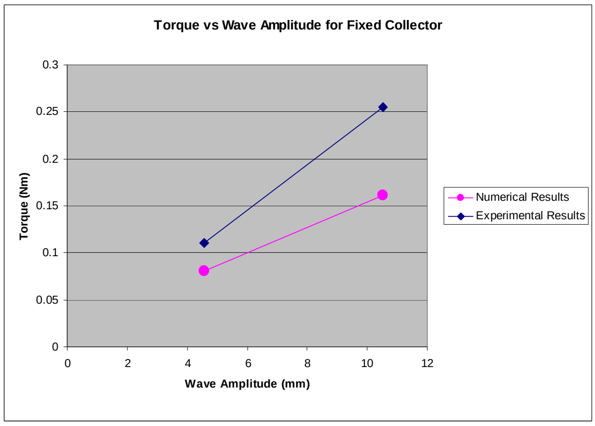

Figure 11: Torque (Nm) vs Wave amplitude (mm) for fixed collector.

The numerically modeled surging response of WRASPA to the incident waves at various instants is shown in Fig. 12. The colour contours in Fig. 12 refer to the velocity profile.

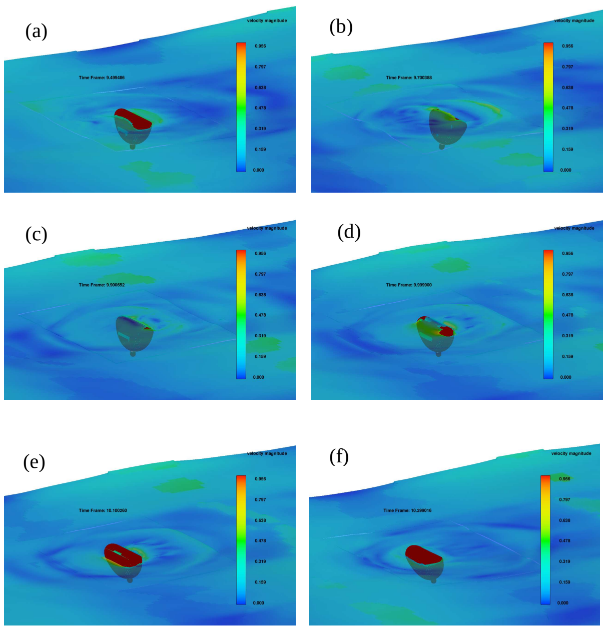

Figure 12: Wave interaction with WRASPA at various time instants.

5 Conclusions and Future Work

Device decay tests were modeled using Flow-3D and the results are in good agreement with experimentally measured data. These tests are used to tune the device shape and the resulting parameters, namely pivot depth and freeboard, are used in the experimental setup. In the characterization tests the resulting torque for a fixed collector body is slightly under-estimated. However, this test has been used to predict output power for two different collector shapes. Further work will concentrate on investigating the cause of the under-estimated torque difference. Numerical results for the pitch motion of WRASPA are in reasonable agreement with the experimental results. Further work will involve an investigation of the pressure profile on the collector body. Another important aspect which requires further investigation is the vorticity generation in the vicinity of the collector so as to improve the optimization of the collector shape.

Acknowledgements

The authors would like to acknowledge funding for this project from the UK Joule Centre (www.joulecentre.org) via Grant Ref No. JIRP306/02.

References

[1] Bracewell RH. Frog and PS Frog (1990). “A study of two reactionless ocean wave energy converters”, *PhD thesis. UK:* Lancaster University.

[2] French M., and Bracewell R. (1995). “The systematic design of economic wave energy converters,” *5th International Offshore and Polar Engineering Conference*, The Hague, June 11-16.

[3] Budal K. and Falnes J. “A resonant point absorber of ocean-wave power, *Nature*, vol. 256 pp. 478-479, 1975.

[4] Evans D.V. “Some analytical results for 2D and 3D wave energy absorber” pp. 213-249 in “*Power from Sea Waves*” Ed Count, B M, Ac. Press 1980.

[5] Chaplin R.V. and Folley M.S (1998). “Sea-bed devices-technical comparisons of existing and new types,” *4th European Wave Energy Conference,* Patras.

[6] Chaplin, R.V. and Aggidis G.A. (2007a). “WRASPA: Wave Interactions and Control in a new Pitching-Surge Point-Absorber Wave Energy Converter,” *7th European wave and tidal energy conference*, Portugal.

[7] Chaplin R.V. and Aggidis G.A (2007b)., “An Investigation into Power from Pitch-Surge Point-Absorber Wave Energy Converters,” published by *IEEE, Clean Electrical Power*, ICCEP '07.

[8] Chaplin R.V. and Aggidis G.A., Rahmati, M.T (2008). “WRASPA: (Wave-driven, Resonant, Arcuate action, Surging Power-Absorber),” *Wave and Tidal Symposium, Renewable Energy Association*, Cardiff, Wales, 2008.

[9] Rahmati M.T., Aggidis G. A. and Chaplin R.V (2008). “Investigating Pitching-Surge Power-Absorber Wave Energy Converters,” *ASME POWER*, Florida, USA, July 2008.

[10] Aggidis G.A., Rahmati M.T., McCabe A.P., Chaplin R.V., Bhinder M.A., Mingham C.G. and Causon D.M. “ Optimum power capture of a new wave energy converter in irregular waves”, *Proceedings of the ASME 28th International Conference on Ocean, 0ffshore and Arctic Engineering,* OMAE2009-79421.

[11] Bhinder M.A., Mingham C.G., Causon D.M., Rahmati M.T., Aggidis G.A. and Chaplin R.V. “ A joint numerical and experimental study of a surging point absorbing wave energy converter (WRASPA)”, *Proceedings of ASME 28th International Conference on Ocean, Offshore and Arctic Engineering*, OMAE2009-79392.

[12] Hirt, C. W. and Nichols, B.D. (1981). “Volume of Fluid (VOF) method for the dynamics of free boundaries,” *J. Comp. Phys*., 39,201-225.

[13] Goldstein H., Charles P. and Safko J., 2002, Classical Mechanics, *Addison Wesley*, Washington.

[14] Flow-3D (2008) *user manual*, *version 9.3*.